Sheet Excitability and Nonlinear Wave Propagation

Bernardo Pando,[1] John E. Pearson,[2] and Silvina Ponce Dawson[1]

[1]*Departamento de Física, FCEN-UBA, Ciudad Universitaria, Pabellón I, (1428) Buenos Aires, Argentina*

[2]*Computational Science Methods MS F645, Los Alamos National Laboratory, Los Alamos, New Mexico 87545, USA*

(Received 7 June 2003; published 16 December 2003)

In the *Xenopus laevis* oocyte, calcium ion channels are clustered in a thin shell. Motivated by this morphology, we study a general class of reaction-diffusion systems that include most of the well-known models that support wave propagation but restricting excitability to a "sheet" of codimension 1. We find waves that undergo propagation failure with *increasing* diffusion coefficient and a scaling regime in which the wave speed is independent of it.

DOI: 10.1103/PhysRevLett.91.258101 PACS numbers: 87.10.+e, 82.33.–z, 87.17.–d

Living organisms use excitable nonlinear waves to transport information. Waves of electrical activation in the heart [1] and of Ca^{2+} release during fertilization [2] are two such examples. Excitability [3,4], a property of various chemical, physical, and biological systems, makes these nonlinear waves possible. The paradigmatic example of excitability is the propagation of action potentials in nerves [5]. In some nerve fibers, the excitability of the medium is not spatially uniform but limited to narrow regions called the *nodes of Ranvier* [6]. This gives rise to saltatory propagation, in which the wave undergoes rapid jumps at the nodes [7]. Cells have evolved to optimize their properties: The wave speed in nerve fibers with nodes is higher than in spatially uniform ones. Ca^{2+} waves, another common cell signaling mechanism [8], can also be saltatory [9–11]. Intracellular Ca^{2+} waves involve Ca^{2+} release from internal stores through Ca^{2+} channels, the subsequent diffusion of Ca^{2+} in the cytosol and the "recapture" by various pumps and buffers. These processes occur in different cell types [2,12,13]. In all of them, the cytosol acts as an excitable medium because the open probability of the Ca^{2+} channels depends on the cytosolic Ca^{2+} concentration, resulting in *calcium induced calcium release* [14]. In most cases, the Ca^{2+} channels are distributed nonuniformly. Consequently, there are various spatially localized Ca^{2+} signals [12,13] and Ca^{2+} waves can be saltatory or continuous [9–11]. We may thus conclude that dynamics and geometry combine to provide the cell with a flexible signaling repertoire.

In this Letter, we consider another geometric property that affects excitable wave propagation. Motivated by the observation that Ca^{2+} channels in the $\sim$1 mm diameter *Xenopus* oocyte lie in a thin shell about 6μ thick [13], we study wave propagation when the excitability of the system is restricted to a sheet of codimension one. This morphology, which has not been previously considered, has ramifications for Ca^{2+} signaling. The more general problem of nonlinear waves generated by sources lying in a lower dimensional space than the embedding medium is also of great physical interest. In this Letter, we first treat this problem using an extension of the fire-diffuse-fire (FDF) model [9–11] of $[Ca^{2+}]$ waves in which the signaling agent diffuses in three-dimensional space but is released from point sources located in a two-dimensional sheet. We also present a general analysis for the case in which the source is continuous over the sheet. Diffusion plays a dual role here. It is necessary for wave propagation but also acts as a sink by removing the signaling agent from the sheet. We thus find waves that undergo propagation failure with increasing diffusion coefficient and an asymptotic regime in which the wave speed is independent of the diffusion coefficient. Waves in homogeneous media do not share these counterintuitive properties.

In the FDF model, clusters of channels are represented by point sources separated by a distance d, which "fire" when the Ca^{2+} concentration at the site reaches a threshold. This last condition is meant to mimic excitability. The sites fire for a time, τ, releasing a total, σ, of Ca^{2+} ions. Ca^{2+} diffuses between clusters with diffusion coefficient, D, on top of a basal concentration, $[Ca^{2+}]_B$. Here we modify the FDF model so that all the release sites are located on the $z = 0$ plane and look for waves that travel in the x direction. As in [11], we consider only the discreteness of release sites in the direction of propagation, treating both the solution and the distribution of release sites as y independent. We define a dimensionless concentration u by dividing the dimensional one ($[Ca^{2+}] - [Ca^{2+}]_B$ in the case of Ca^{2+}) by the threshold concentration, u_c, and dimensionless space and time coordinates, $x \to x/\lambda$, $z \to z/\lambda$, and $t \to Dt/\lambda^2$, with λ a distance scale that we discuss later. In these variables, the evolution equation reads

$$\frac{\partial u}{\partial t} = \frac{\partial^2 u}{\partial x^2} + \frac{\partial^2 u}{\partial z^2} + \Lambda\delta(z) \times \sum_{i=-\infty}^{+\infty} \delta\left(x - i\frac{d}{\lambda}\right) H(t - t_i) H\left(t_i + \frac{D\tau}{\lambda^2} - t\right), \quad (1)$$

where H is the Heaviside function [$H(x) = 0$, for $x \leq 0$ and 1 for $x > 0$], $\Lambda \equiv d/\ell$, and t_i is the minimum time, t, such that $u(x_i, z = 0, t) = 1$. The length scale d is the separation between the release sites, and

$$\ell \equiv D u_c d^2 \tau/\sigma. \quad (2)$$

In order to minimize the number of parameters, we either set $\lambda = d$ or $\lambda = \ell$. In both cases, the resulting evolution equation depends only on $\beta = D\tau/d^2$ and Λ. In what follows, we will take $\lambda = d$ except in the limiting case $\Lambda \to 0$ in which case we take $\lambda = \ell$.

We seek propagating solutions such that $t_i = x_i/c$ with c a dimensionless constant velocity. This does not mean that the solution propagates without deformation, but that the time interval between adjacent firings is unchanging. The formal solution to Eq. (1) for $t_{-1} < t \le 0$ and $c > 0$, at $x = 0$, $z = 0$, is $u(0,0,t) = \sum_{i=-\infty}^{-1} \frac{\Lambda}{4\pi} \int_{x_i/c}^{\min[t,(x_i/c)+\beta]} \times [(dt')/(t-t')] \exp\{-[x_i^2/4(t-t')]\}$. Given β and Λ, $u(0,0,0)$ is a function of c:

$$f(c) \equiv u(0,0,0) = \frac{\Lambda}{4\pi}\left[\sum_{n>[\beta c]}^{\infty} \mathrm{Ei}(-q_n) - \sum_{n=1}^{\infty} \mathrm{Ei}(-p_n)\right], \quad (3)$$

where $\mathrm{Ei}(-x) = \int_x^\infty dt\, e^{-t}/t$, $p_n \equiv nc/4$, and $q_n \equiv (n^2 c)/(4n - 4c\beta)$. Since $u(0,0,0) = 1$, then $c = f^{-1}(1)$ with c depending on Λ and β. Figure 1(a) is a plot of $f(c)/\Lambda$ vs c for different values of β. We see that $f(c)/\Lambda$ has a maximum, $A(\beta)$, for all values of β. Therefore f^{-1} exists only in the region of the $\Lambda - \beta$ parameter space where $1 \le \Lambda A(\beta)$. Figure 1(b) is a plot of $A(\beta)$ in which it is shown that for a given value of β there is a solution to $f(c) = 1$ for $\Lambda > \Lambda_{\min}(\beta)$ with $\Lambda_{\min}(\beta)$ a decreasing function of β. As shown in Fig. 1(b), we can approximate the curve by simple scaling relationships over certain intervals. We can also observe in Fig. 1(a) that, for the allowed values of Λ and β, $f^{-1}(1)$ has two values. Only the one that corresponds to the largest c (or to the minimum time at which $u = u_c$ at the site) is the traveling wave solution. The existence of another c value that satisfies $f(c) = 1$ is related to the fact that $u = u_c$ twice at each release site, once on the way up and once on the way down. The same behavior is observed in the original FDF model only when pumps that remove Ca^{2+} are taken into account [9].

As in the original FDF model, the discreteness of the release sites is either manifest or not, depending on the value of β, as shown in Fig. 2. These plots display the solutions in the traveling frame ($\xi \equiv x - ct$), with c obtained by solving $f(c) = 1$. In the original model, the traveling pulse left a high concentration behind. In the current case, the solution decays to zero far behind the traveling front because diffusion removes the signaling agent from the excitable region (i.e., the sheet $z = 0$). This is similar to the behavior of the original FDF model when pumps are included.

The wave velocity scales differently with D depending on whether the propagation is saltatory or continuous. This can be seen from Fig. 3, where we plot $v\tau/d$, with v the dimensional velocity of the wave, as a function of β for various values of $\Lambda\beta$. Taking $\Lambda\beta$ fixed while varying β is equivalent to varying only the diffusion coefficient, D. Thus, the scaling of $v\tau/d$ vs β is the same as the scaling of v vs D. We can deduce from Fig. 3 that $v \sim D$ for small enough β. This corresponds to the extremely saltatory case and the scaling is similar to the one of the usual FDF model. As D is increased, the slope of the curve decreases and the velocity reaches a maximum value. Eventually the traveling wave solution ceases to exist. The end points of the curves at large values of D correspond to the disappearance of the solution. The occurrence of propagation failure with increasing D is not observed in the usual FDF model and is a consequence of the role of diffusion as a sink: The larger D the more efficient the sink is, and this eventually leads to the disappearance of the solution. More surprisingly, for large enough $\Lambda\beta$, the curve displays a plateau spanning several decades in D. Thus, there is a regime in which the velocity

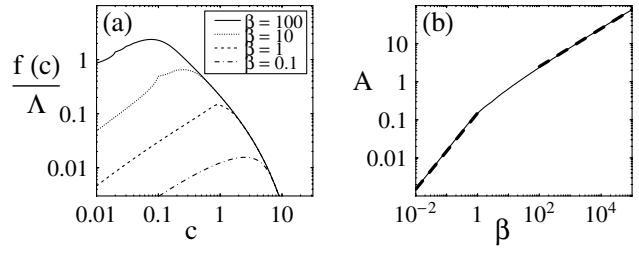

FIG. 1. (a) $f(c)/\Lambda$ for various β. (b) The maximum value of $f(c)/\Lambda$, A, as a function of β. The dashed lines are the approximations $A \approx \beta/6$ and $A \approx .25\beta^{1/2}$ for small and large β, respectively.

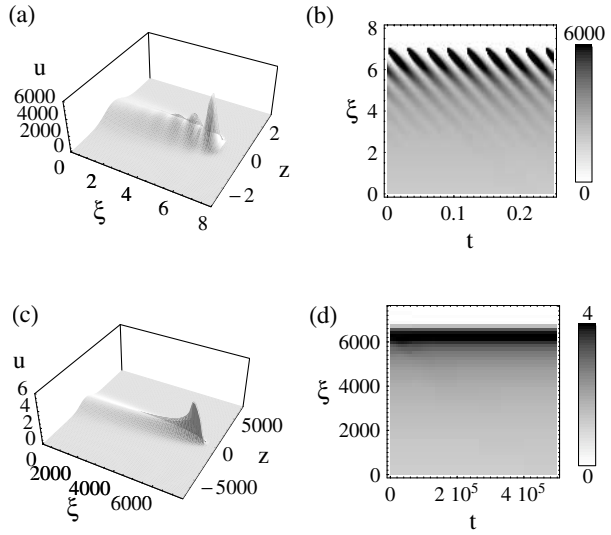

FIG. 2. Profile of u as a function of $\xi \equiv x - ct$ and t [(a),(c)] and corresponding space-time plots along the ξ axis [(b),(d)] for $\beta = 0.001$, $\Lambda = 2 \times 10^6$ [(a),(b)] and $\beta = 50000$, $\Lambda = 0.04$ [(c),(d)]. The speed is $c = 33.9$ in (a),(b) and $c = 0.0126$ in (c),(d). The propagation is saltatory in (a),(b) and continuous in (c),(d). These plots were made with finite spatial resolution thus mimicking real data.

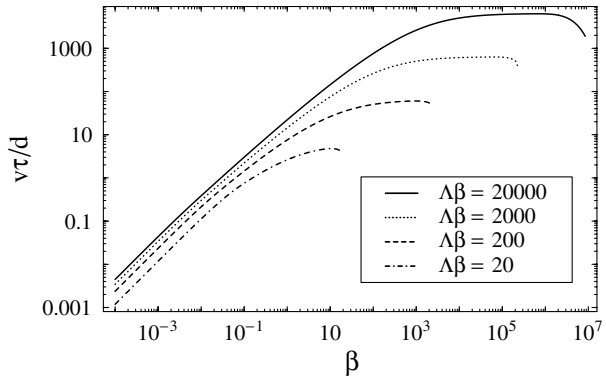

FIG. 3. $v\tau/d$ as a function of $\beta = D\tau/d^2$ for $\Lambda\beta = \sigma/(u_c d^2) = 20, 200, 2000, 20\,000$.

of the wave, which propagates solely by diffusion, is independent of the diffusion coefficient. This surprising result is again due to the role of diffusion as a sink. This behavior takes place in the continuum limit, and we will show that it occurs in more general cases.

There are two limits in which the v dependence on D can be deduced with simple scaling arguments. The extreme saltatory case corresponds to the limit $\beta \to 0$, $\Lambda \to \infty$ while the product $\Lambda\beta = \sigma/(u_c d^3) \equiv \Gamma$ remains finite. For these values of β, $A(\beta) \approx \beta/6$, so that $\Lambda\beta > 6$ in order for the traveling wave solution to exist. In the saltatory limit, Eq. (1) becomes

$$\frac{\partial u}{\partial t} = \frac{\partial^2 u}{\partial x^2} + \frac{\partial^2 u}{\partial z^2} + \Gamma\delta(z) \sum_{i=-\infty}^{+\infty} \delta(x - i)\delta(t - t_i), \quad (4)$$

where $u(i, 0, t_i) = 1$. The boundary conditions are $u \to 0$, as $|x|, |z| \to \infty$ so that c is a function of Γ only. The dimensional velocity is

$$v = c(\Gamma)\frac{D}{d}, \quad (5)$$

which explains the linear scaling in the small β region of Fig. 3.

In the original FDF model, the continuum limit corresponds to $d/\sqrt{D\tau} \to 0$ and σ/d^3 finite, so that the sum of δ functions over active release sites can be replaced by an integral. In the present case, the continuum limit corresponds to $\Lambda \to 0$ and σ/d^2 finite. Then the sum on the right-hand side of Eq. (1) (with $\lambda = \ell$) becomes an integral over the active sites along the direction of propagation x and a two-dimensional release density over the $z = 0$ plane, σ/d^2, exists. In this way ℓ remains finite even though $d \to 0$. Taking the limit and nondimensionalizing Eq. (1) with $\lambda = \ell$ yields

$$\frac{\partial u}{\partial t} = \frac{\partial^2 u}{\partial x^2} + \frac{\partial^2 u}{\partial z^2} + \delta(z)H(x - \hat{x}_1)H(\hat{x}_2 - x). \quad (6)$$

Here $\hat{x}_2$ and $\hat{x}_1$ are functions of time defined implicitly through $u(\hat{x}_2, t) = 1$ and $u(\hat{x}_1, t - \Lambda^2\beta) = 1$. Thus, $\hat{x}_2$ and $\hat{x}_1$ delimit the region with active sites. For the traveling wave solution, these spatial points travel with the wave at speed $\tilde{c}$ so that the dimensionless front width is $\hat{w} \equiv \hat{x}_2 - \hat{x}_1 = \tilde{c}\Lambda^2\beta$ [15]. The traveling wave solution is further characterized by the boundary conditions: $u \to 0$, $|x|$, $|z| \to \infty$. Since Eq. (6) depends only on $\Lambda^2\beta$ and given the boundary conditions, it follows that the dimensionless velocity, $\tilde{c}$, is a function of $\Lambda^2\beta$. The dimensional velocity, v, is then given by

$$v = \frac{D}{\ell}\tilde{c}(\Lambda^2\beta) = \frac{\sigma}{u_c\tau d^2}\tilde{c}(\Lambda^2\beta). \quad (7)$$

As previously mentioned, for small Λ, there is a traveling wave solution only for large enough β. In that region of β values, $A(\beta) \approx 0.25\sqrt{\beta}$ (see Fig. 1). Thus, $\Lambda^2\beta > 16$ in order for the traveling wave solution to exist. Now, if $\Lambda^2\beta \gg 1$ then $\hat{w} \gg 1$, i.e., the trailing edge of the active region is far from the leading edge. Then $\tilde{c}$ becomes insensitive to $\Lambda^2\beta$. From Eq. (7), it then follows that v is effectively independent of D in this limit, which explains the plateau in Fig. 3. This result is also easy to derive from the expression $f(\tilde{c})$ in the continuum limit. The existence of the additional length scale, ℓ, is ultimately responsible for the occurrence of this peculiar behavior in which a diffusion-driven wave travels at a speed that is independent of the diffusion coefficient.

We now show that the existence of diffusion-driven waves with a D-independent velocity is a general feature of reaction-diffusion systems in which diffusion occurs in the full space while the reactions are restricted to a codimension one "sheet." Consider, for example, a bistable reaction-diffusion system of the form $\tilde{u}_{\tilde{t}} = D\tilde{\nabla}^2\tilde{u} + \delta(\tilde{z})(LU/T)f(\tilde{u})$, where all variables are dimensional with the exception of f, which is assumed to be dimensionless. In that way L, U, and T are parameters that give the right dimensions of the "reaction term," the presence of the $\delta(\tilde{z})$ indicates that it is different from zero only on the $z = 0$ plane and the product UL is a two-dimensional density on that plane (e.g., in the FDF model these parameters correspond to $L = \sigma/u_c d^2$, $U = u_c$, $T = \tau$). If this system possesses a traveling wave solution that tends to a fixed point of f as $x, z \to \pm\infty$, its velocity is independent of D. To show this, we define dimensionless variables: $u \equiv \tilde{u}/U$, $x \equiv \tilde{x}/\lambda$, $z \equiv \tilde{z}/\lambda$, $t \equiv D\tilde{t}/\lambda^2$ with $\lambda = DT/L$. Then the evolution equation becomes $u_t = \nabla^2 u + \delta(z)f(Uu)$ which implies that the dimensionless velocity c does not depend on D. It follows that the dimensional velocity v is D independent: $v = Dc/\lambda = Lc/T$. The same result applies if u and f are vectors instead of scalars. A somewhat similar result is obtained for two-variable excitable systems of the form $\tilde{u}_{\tilde{t}} = D\tilde{\nabla}^2\tilde{u} + \delta(\tilde{z})(LU/T)f(\tilde{u}, \tilde{h})$, $\tilde{h}_{\tilde{t}} = (H/T')g(\tilde{u}, \tilde{h})$ with a single spatially homogenous stationary solution. Systems of this type include the two-variable reduction of the Hodgkin-Huxley model [7] (i.e., the FitzHugh-Nagumo model), or of the DeYoung-Keizer model of intracellular Ca^{2+} dynamics [14,16], when the ion channels are restricted to the $z = 0$ plane. Proceeding

as before (with $h = \tilde{h}/H$), we obtain the dimensionless equations $u_t = \nabla^2 u + \delta(z) f(Uu, Hh)$, $h_t = (DT^2/L^2T') \times g(Uu, Hh)$. In this case, if there is a pulse that tends to the fixed point of the system as $x, z \to \pm\infty$, the dimensionless solution, in principle, depends on D. However, if $DT^2/(L^2T') \ll 1$, then we may assume that h is approximately constant while v varies significantly. In this limit, which holds if D is not too large, the dimensionless traveling pulse solution and the dimensional velocity are D independent. This is a consequence of the behavior we found for the bistable case, since in this limit the front dynamics can be described, as usual, replacing the excitable system by a bistable one [7]. On the other hand, if D is large enough, we expect propagation failure as in the continuum limit of the FDF model.

We now use the FDF model to give heuristic explanations for the scalings discussed in this Letter. Fick's law states that diffusive fluxes are given by $D\nabla u$. Thus, a mean velocity can be defined as $v \sim D/L_u$ with L_u a characteristic length scale of variation of u. In order to estimate L_u, we need to distinguish between continuum and saltatory propagation. In the saltatory case, sites are distinguishable and $L_u = d$. Thus, $v \sim D/L_u = D/d$. In the continuum case, sites begin to fire when they are on the edge of the active region which is effectively a source of u. Then, we estimate L_u using the diffusion equation in the presence of a source, s: $\partial u/\partial t = s + D\nabla^2 u$ and considering its stationary solution $s = -D\nabla^2 u$. Thus, we can estimate $L_u \sim \sqrt{Du/s}$, with u a characteristic concentration. At the leading edge, $u = u_c$, so $L_u = \sqrt{Du_c/s}$. It then follows that the speed of propagation goes as $v \sim D/L_u = \sqrt{Ds/u_c}$. In the original FDF model, the source is uniformly distributed along the front and $s = \sigma/(d^3\tau)$. Thus, $L_u = \sqrt{Du_c d^3\tau/\sigma} = \sqrt{D\tau/\Gamma}$ and the speed scales as $v \sim D/L_u = \sqrt{\Gamma D/\tau}$. In the model discussed in this paper, the source is localized: $s = \sigma\delta(z)/(d^2\tau)$. For this calculation, we will consider it to be spread over width L_u in the z direction so that $s = \sigma/(d^2 L_u \tau)$. Now, since $L_u = \sqrt{Du_c/s} = \sqrt{Du_c d^2 L_u \tau/\sigma}$, we get $L_u = Du_c d^2\tau/\sigma = \ell$. Thus, because of the diffusive spread in the direction perpendicular to the plane of release sites, $L_u = \ell \sim D$ and $v \sim D/\ell = \sigma/(u_c d^2\tau)$ is independent of D. The limit in which $v \sim D/\ell$ requires that $d \ll \ell$ and $\Lambda^2\beta = D\tau/\ell^2 \gg 1$, which is equivalent to $d \ll \ell \ll w \equiv \hat{w}\ell$. This means that the active region needs to be very large to sustain the wave which is depleted by diffusion. In the original FDF model, propagation failure occurs when the ratio of the release density, σ/d^3, to the excitability threshold, u_c, is not large enough. In the current model, propagation failure also occurs when a ratio of release density to threshold ($\Lambda^2\beta = \sigma/(u_c d^2\sqrt{D\tau})$ is not large enough but now with a release density that accounts for the spread of the signaling agent over a distance $\sqrt{D\tau}$ while the site is active.

In systems that are excitable in a sheet of lower dimensionality than the embedding space, diffusion plays a dual role, serving as both transport mechanism and as a sink by removing the signaling agent from the excitable sheet. Waves in homogeneous media do not share these properties. Inhomogeneities imply the possibility of additional wave-speed scalings beyond the $D^{1/2}$ one considered in the biological literature [17]. The cell is a complex place; it would be surprising were it to single out the trivial square root scaling. We have demonstrated wave speeds that scale as $v \sim D^\eta$ for all η in $0 \le \eta \le 1$. In particular, we can expect $v \sim D^0$ to occur whenever the sheet of excitability is of codimension 1. We have not analyzed the codimension $q \neq 1$ problem in detail, but it seems likely that other unexpected scalings will be encountered.

Part of this work was performed at the Santa Fe Institute. We thank them for their hospitality. The work was additionally supported by NIH Grant No. 1RO1GM65830-01, UBA, and ANPCyT-Argentina (PICT 03-08133).

[1] L. Glass, Phys. Today **49**, No. 8, 40 (1996).
[2] R. A. Fontanilla and R. Nuccitelli, Biophys. J. **75**, 2079 (1998); J. Wagner, Y. X. Li, J. Keizer, and J. E. Pearson, Biophys. J. **75**, 2088 (1998).
[3] S. Alonso, F. Sagues, and A. S. Mikhailov, Science **299**, 1722 (2003).
[4] J. E. Pearson, Science **261**, 189 (1993); K. Lee, W. McCormick, J. E. Pearson, and H. L. Swinney, Nature (London) **369**, 215 (1994); W. N. Reynolds, J. E. Pearson, and S. Ponce-Dawson, Phys. Rev. Lett. **72**, 2797 (1994).
[5] A. L. Hodgkin and A. F. Huxley, J. Physiol. **116**, 449 (1952).
[6] D. J. Aidley, *The Physiology of Excitable Cells* (Cambridge University Press, Cambridge, England, 1998), pp. 49–52.
[7] J. Sneyd and J. Keener, *Mathematical Physiology* (Springer, New York, 1998).
[8] M. J. Berridge, M. D. Bootman, and P. Lipp, Nature (London) **395**, 645 (1998).
[9] J. Keizer, G. D. Smith, S. Ponce-Dawson, and J. E. Pearson, Biophys. J. **75**, 595 (1998).
[10] J. E. Pearson and S. Ponce-Dawson, Physica (Amsterdam) **257A**, 141 (1998).
[11] S. P. Dawson, J. Keizer, and J. E. Pearson, Proc. Natl. Acad. Sci. U.S.A. **96**, 6060 (1999); http://www-xdiv.lanl.gov/XCM/pearson/skid_row_relay.ps; http://www-xdiv.lanl.gov/XCM/pearson/fdf/
[12] H. Cheng, W. J. Lederer, and M. B. Cannell, Science **262**, 740 (1993).
[13] N. Callamaras and I. Parker, J. Gen. Physiol. **113**, 199 (1999).
[14] G.W. De Young and J. Keizer, Proc. Natl. Acad. Sci. U.S.A. **89**, 9895 (1992).
[15] We define $\tilde{c} = v\ell/D$ to distinguish it from $c = vd/D$.
[16] Y.-X. Li and J. Rinzel, J. Theor. Biol. **166**, 461 (1994).
[17] L. F. Jaffe, Cell Calcium **14**, 736 (1993); Proc. Natl. Acad. Sci. U.S.A. **88**, 9883 (1991).